ELSEVIER

International Journal of Mass Spectrometry 188 (1999) 131–146

International Journal of Mass Spectrometry

Relationship between in-source and post-source fragment ions in the matrix-assisted laser desorption (ionization) mass spectra of carbohydrates recorded with reflectron time-of-flight mass spectrometers

David J. Harvey[a,*], Ann P. Hunter[a], Robert H. Bateman[b], Jeff Brown[b], Glen Critchley[b]

[a]*Department of Biochemistry, Oxford Glycobiology Institute, South Parks Road, Oxford OX1 3QU, UK*
[b]*Micromass Ltd., Floats Road, Wythenshawe, Manchester M23 9LZ, UK*

Received 13 August 1998; accepted 4 December 1998

Abstract

The reflectron matrix-assisted laser desorption (ionization) [MALD(I)] mass spectra of many complex carbohydrates (and other compounds) recorded with time-of-flight (TOF) instruments fitted with time-lag focusing (delayed extraction) contain focused fragment ions resulting from fragmentation within the ion source, together with unfocused (metastable) fragments derived from post-source decay. The latter ions are particularly abundant from carbohydrates containing sialic acids as the result of loss of the sialic acid moieties. The relative abundance of these metastable ions was found to decrease with ion-source pulse delay whereas the mass difference between the focused and unfocused ions increased. The mass difference was also found to vary with the instrument used to record the spectra. An equation has been derived that links the masses of the precursor ion with the two fragment ions (focused and unfocused). It contains a term reflecting the geometry of the mass spectrometer and can, thus, be used with any TOF instrument. The formula can be rearranged such that the mass of an absent molecular ion can be predicted from the masses of the two fragment ion peaks. The metastable ions can also be used to confirm fragmentation pathways in the manner similar to that used for spectra recorded with magnetic sector instruments. Metastable ions were also found in spectra recorded with an orthogonal-TOF mass spectrometer using field ionization. The formulae relating the masses of the fragment and precursor ions were also found to apply in this case, further demonstrating their instrument independence. (Int J Mass Spectrom 188 (1999) 131–146) © 1999 Elsevier Science B.V.

Keywords: matrix-assisted laser desorption (ionization) [MALD(I)], Carbohydrates; Fragment ions; Post-source decay; Metastable ions

1. Introduction

Matrix-assisted laser desorption (ionization) [MALD(I)] mass spectrometry was first introduced for the analysis of N-linked carbohydrates by Mock et al. in 1991 [1] and has also proved to be valuable for the analysis of other carbohydrate-containing compounds such as glycolipids [2,3]. Several reviews have appeared (e.g. [4–6]). Spectra are characterised by abundant MNa^+ ions from most matrices [1,7,8] with 2,5-dihydroxybenzoic acid (2,5-DHB) [9] generally being the matrix of choice. In addition to

* Corresponding author. E-mail: dh@glycob.ox.ac.uk

Dedicated to Brian Green for his many innovative contributions to mass spectrometry instrument development and for his tireless help in teaching us how to take advantage of them.

PII S1387-3806(99)00014-7

MNa^+, the reflectron-TOF MALD(I) spectra of many carbohydrates and other compounds show several well focused fragment ions, particularly when recorded with instruments fitted with time-lag focusing (delayed extraction). These ions have previously been shown to be the result of in-source fragmentation [10] and are particularly abundant in the spectra of sugars containing sialic acid groups where they are formed by loss of the sialic acid moiety. In addition to these focused, in-source, fragment ions, several poorly focused ions are often also present at masses slightly higher than those of the in-source fragments. These latter, metastable, ions are formed by the same fragmentation as that producing the in-source fragments but in the first field-free region of the instrument and are those normally focused in post-source decay (PSD) experiments [11–16]. The relative abundance and apparent mass of these metastable ions varies with the ion source focusing conditions and with the instrument used to record the spectra. This article investigates these relationships and presents a formula linking the masses of the precursor ion with those of the focused and unfocused fragments.

2. Experimental

2.1. Materials

Neutral oligosaccharides were obtained from Oxford GlycoSciences Ltd. (Abingdon, Oxfordshire, UK). The di-sialylated biantennary glycan was from Dextra Laboratories Ltd. (Reading, UK). Glycolipids were from Sigma Chemical Co., Ltd. (Poole, Dorset, UK). Ovalbumin sugars were released from chicken ovalbumin (Sigma grade V) by hydrazinolysis and reacetylated [17]. 2,5-DHB and α-cyano-4-hydroxycinnamic acid (4-HCCA) were purchased from Aldrich Chemical Co. (Gillingham, Dorset, UK) and were used without further purification.

2.2. Sample preparation

The oligosaccharides (50–100 pmole), dissolved in water (1 μl), were mixed with the matrix solution (1 μl of a saturated solution of 2,5-DHB or 4-HCCA in acetonitrile) on the mass spectrometer target and allowed to dry at room temperature. The dried mixture from 2,5-DHB was then recrystallised from ethanol (about 1 μL) to provide a more homogeneous sample surface [18].

2.3. Mass spectrometers and spectral acquisition

Spectra were recorded with Micromass TOFSpec 2E and SE mass spectrometers, and a PerSeptive Biosystems Voyager Elite Reflectron-TOF instrument, all utilising nitrogen lasers (337 nm). The instruments were operated with an extraction voltage of 20 kV and calibrated with glycans from chicken ovalbumin. For the experiments investigating the effect of delay on the metastable ion mass and relative abundance, the delay was varied between the lower limit provided by the instrument and the point at which the metastable ion could no longer be observed. For each delay, the pulse (TofSpec 2E) or grid voltage (Voyager) was adjusted in order to focus the fragment ion and the instrument was recalibrated.

The PSD spectrum of $(Man)_6(GlcNAc)_2$ from chicken ovalbumin was recorded with the Micromass 2E instrument. The sample (0.5 μL), containing the whole range of ovalbumin glycans [8] was loaded at a concentration of 200 pmol/μL and the ion of mass-to-charge ratio 1420.2 was selected. The laser power was increased to 80% (144 μJ) of maximum and 25 laser shots were fired at each of 12 segments covering the whole mass range. Three complete cycles of the mass range were made and all data were averaged using the Micromass MassLynx data system.

The positive ion field ionization (FI) spectrum of $C_{14}H_{30}$ was recorded with an experimental Micromass orthogonal TOF mass spectrometer. Sample introduction was from a 200 ng/μl solution injected into a 30 m $\times$ 250 μm inner diameter (i.d.) fused-silica GLC column (film thickness 0.25 μm). The instrument incorporated a reflectron giving an effective path length of 1.2 m and the drift tube was held at a potential of -4 kV. Spectra were acquired with a

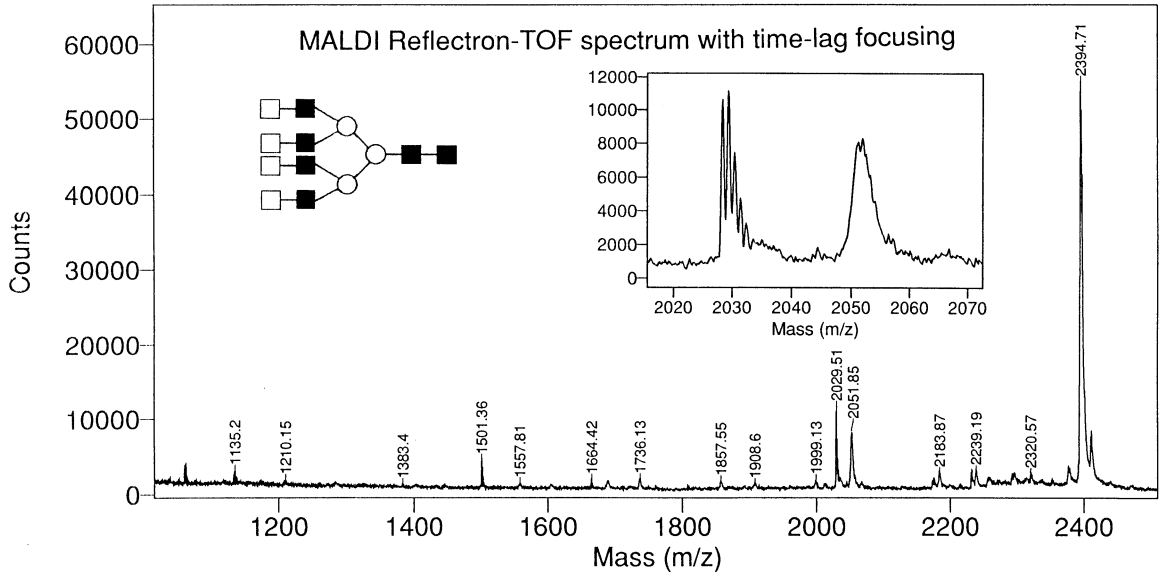

Fig. 1. Positive ion MALD(I) mass spectrum of the biantennary carbohydrate I recorded from 2,5-DHB with the Voyager instrument showing the focused (*m/z* 2029.5) and unfocused (*m/z* 2051.8) fragment ion produced by loss of Gal-GlcNAc. The inset shows these ions on an expanded scale. Filled squares are GlcNAc; open squares are galactose; open circles are mannose.

pulse frequency of 40 kHz to give a mass range of 400 mass units and were digitised at 1 GHz.

3. Results and discussion

Fig. 1 shows the reflectron-TOF MALD(I) mass spectrum of the tetra-antennary oligosaccharide NA4 (Compound 1, Fig. 2) recorded from 2,5-DHB with a 250 ns delay (100 pmoles were loaded onto the target). The abundant MNa^+ ion was accompanied by a number of less abundant in-source fragment ions of which that at *m/z* 2029.5 was due to loss of a nonreducing terminal Gal-GlcNAc residue. This fragment ion was accompanied by the unfocused PSD ion at *m/z* 2051.8.

Fig. 3 shows the more complex positive ion MALD(I) spectrum of the ganglioside GM_1 (II) recorded from 4-HCCA with a short delay (220 ns) to illustrate the very abundant metastable ions (*m/z* 1296.5 and 1324.5) associated with loss of sialic acids from the gangliosides when using this matrix to give the fragments at *m/z* 1277.6 and 1305.6. The sample contained two homologous gangliosides containing C_{18} and C_{20} sphingosine chains, thus giving rise to the two sets of peaks. Although 4-HCCA is a "hotter" matrix than 2,5-DHB in that it normally catalyses the production of more abundant fragment ions, the corresponding metastable ions from this ganglioside were almost as intense when recorded from 2,5-DHB. The complex molecular ion region reflects the presence of the two homologous gangliosides. Thus, the MNa^+ ions from the free acids were at *m/z* 1568.6 and 1596.6 and those from the mono-sodium salts were at *m/z* 1590.6 and 1618.6. Potassium-containing ions of low abundance were also present 16 mass units higher. The ions at *m/z* 1524.7 and 1552.7 (first isotopes labeled) are fragments produced by loss of carbon dioxide. No prominent metastable ions were seen for this fragmentation, probably reflecting a more rapid, in-source reaction.

3.1. Effect of delay time on the relative abundance of the focused fragment ion

Increasing the delay caused an increase in the abundance of the focused fragment relative to that of

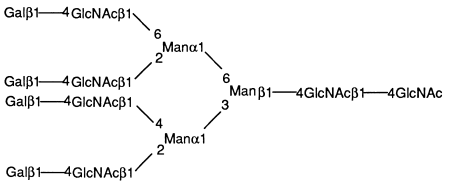

I, Tetra-antennary N-linked glycan

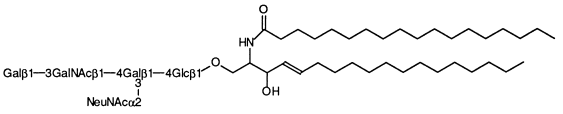

II, Ganglioside G_{M1} (C_{18} sphingosine and C_{18} acyl groups)

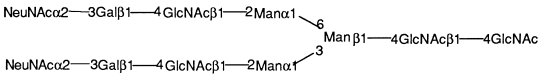

III, Disialylated N-linked biantennary glycan

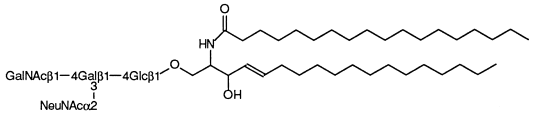

IV, Ganglioside G_{M2}

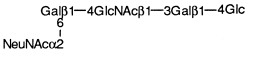

V, Sial-lactose-neo-tetraose (LST)

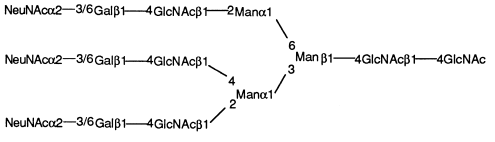

VI, Trisialylated N-linked triantennary glycan

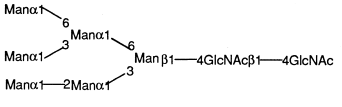

VII, High mannose glycan $(Man)_6(GlcNAc)_2$

Fig. 2. Structures of the carbohydrates and related compounds discussed in this article.

the precursor ion as shown for the tetra-antennary glycan I in Fig. 4. This effect, as described earlier [10], is due to increased time for fragmentation within the ion source and indicates that the rate of this reaction is such that fragmentation occurs in a time frame comparable to the delay time.

3.2. Effect of delay time on the relative abundance of the metastable ion

Fig. 5 shows the effect of varying the delay on the abundance of the metastable PSD ion relative to that of the focused fragment for the tetra-antennary glycan I. Increasing the delay reduced the relative abundance of the metastable ion as more fragmentation occurred within the ion source, as described above. Thus, for maximum PSD efficiency, the delay and, therefore, the ion source residence time should be short in order to minimise the amount of fragmentation occurring within the ion source. A plot of the abundance of the metastable ion relative to that of the in-source fragment as a function of delay time is shown in Fig. 6.

3.3. Effect of delay on the mass separation between the ISD and PSD ions

As the delay was increased, the mass separation between the ISD and PSD ions (ΔM) also increased, as shown in Fig. 7, after the ion source was focused for optimal resolution at each delay setting. This effect was independent of compound type, matrix, or ion polarity and was common to spectra recorded with all instruments although ΔM was different in the various mass spectrometers for the same fragmentation.

3.4. Relationship between the mass of the metastable and fragment ions

Because of the variation of ΔM with ion source focusing conditions, the mass of the metastable ion could not be used with a simple formula (such as $M^* = (M_{frag})^2/M_{precursor}$ [19]), as in spectra recorded with a single focusing magnetic sector instrument, to link a fragment with its precursor ion. However,

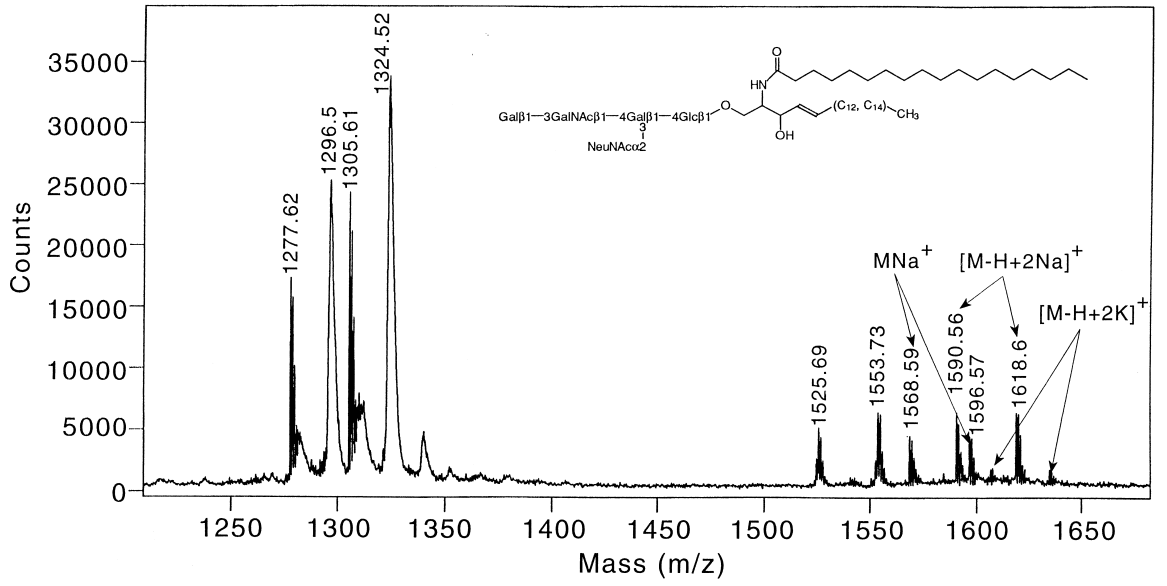

Fig. 3. Positive ion MALD(I) mass spectrum of the ganglioside GM_1 (II) recorded with the Voyager instrument from 4-HCCA. Metastable ions are present at *m/z* 1296.5 and 1324.5. Two compounds are present, containing 18 and 20 carbon atoms in the sphingosine chain.

because the metastable ion was always observed close to the focused fragment, its presence was extremely useful diagnostically, both for identifying an ion as a fragment, and for predicting its origin. The appearance of a metastable ion was particularly valuable in the spectra of mixtures of sugars such as, for example, N-linked glycans released from glycoproteins in which there could be coincidence of mass between a fragment ion formed by glycosidic cleavage and a native sugar. Both of the fragmentations shown above (loss of Gal-GlcNAc or sialic acid) are Y-type cleavages (Domon and Costello nomenclature [20]) (Fig. 8) that leave a free hydroxyl group at the site of cleavage resulting in an ion that is isobaric with a native glycan.

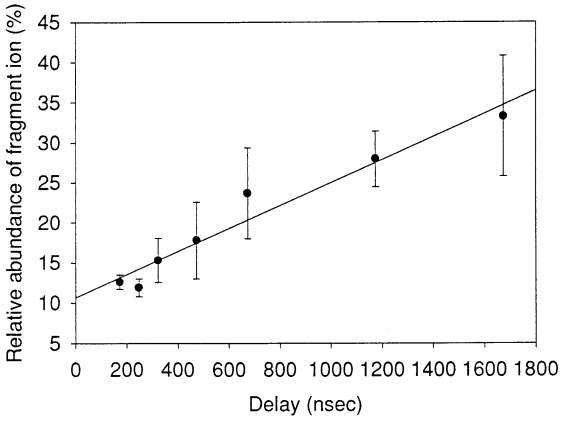

Fig. 4. Graph showing the increase in peak height of the focused fragment ion relative to that of the precursor ion for the tetra-antennary glycan I recorded from 2,5-DHB. Error bars are ± standard deviation.

3.4.1. Derivation of a formula linking the masses of the precursor and fragment ions

Fig. 9 shows the relative electrical potentials versus path length for a typical reflectron-TOF mass spectrometer. Using these potentials, an equation relating the masses of the precursor and the two fragment ion peaks was derived as follows:

$$M_a = M_b + M_n$$

where M_a is the precursor ion, M_b is the fragment ion, and M_n is the neutral loss. The flight time for the precursor ion, T_a, is given by

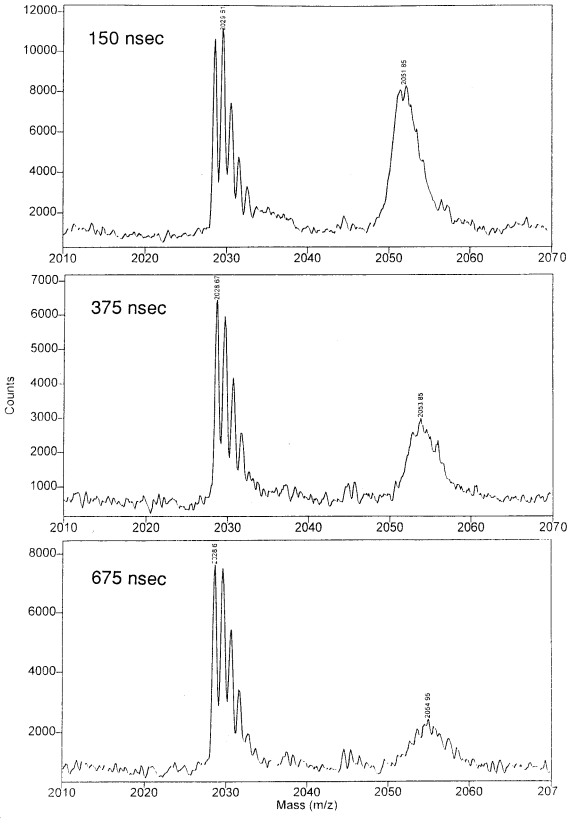

Fig. 5. Expanded view of the focused and unfocused fragment ions due to loss of Gal-GlcNAc from the tetra-antennary glycan I in 2,5-DHB for three different ion-source delay times.

$$T_a = k\sqrt{\frac{M_a}{V}}\,(a_1 s_1 + a_2 s_2 + s_3 + 2s_4 + s_5)$$

where V is ion velocity, a is voltage gradient, and s is distance as defined in Fig. 9. The flight time for the fragment ion formed in the ion source, T_b is given by

$$T_b = k\sqrt{\frac{M_b}{V}}\,(a_1 s_1 + a_2 s_2 + s_3 + 2s_4 + s_5)$$

The flight time for the fragment ion formed in the "field-free region" as a "post-source decay" ion T_c is given by

$$T_c = k\sqrt{\frac{M_a}{V}}\left[a_1 s_1 + a_2 s_2 + s_3 + 2s_4\left(\frac{M_b}{M_a}\right) + s_5\right]$$

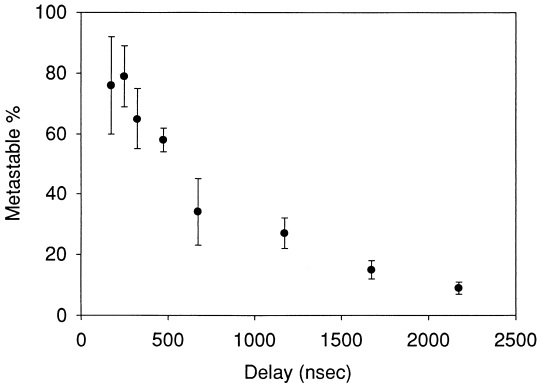

Fig. 6. Graph showing the drop in abundance of the metastable ion relative to that of the focused fragment due to loss of Gal-GlcNAc from the tetra-antennary glycan I as a function of delay. Error bars are ± standard deviation.

The mass assigned to the precursor ion, M_a, is given by

$$M_a = bT_a^2$$

(where b is a calibration constant).

The mass assigned to the fragment ion, M_b, is given by

$$M_b = bT_b^2$$

The mass assigned to the "post-source decay" ion, M_c, is given by

$$M_c = bT_c^2$$

Therefore, the mass assigned to the metastable ion:

$$M_c = M_a\left(\frac{T_c}{T_a}\right)^2$$

substituting for T_c and T_a:

$$M_c = M_a\left[\frac{a_1 s_1 + a_2 s_2 + s_3 + 2s_4\left(\frac{M_b}{M_a}\right) + s_5}{a_1 s_1 + a_2 s_2 + s_3 + 2s_4 + s_5}\right]^2$$

If

$$p = a_1 s_1 + a_2 s_2 + s_3 + s_5$$

and

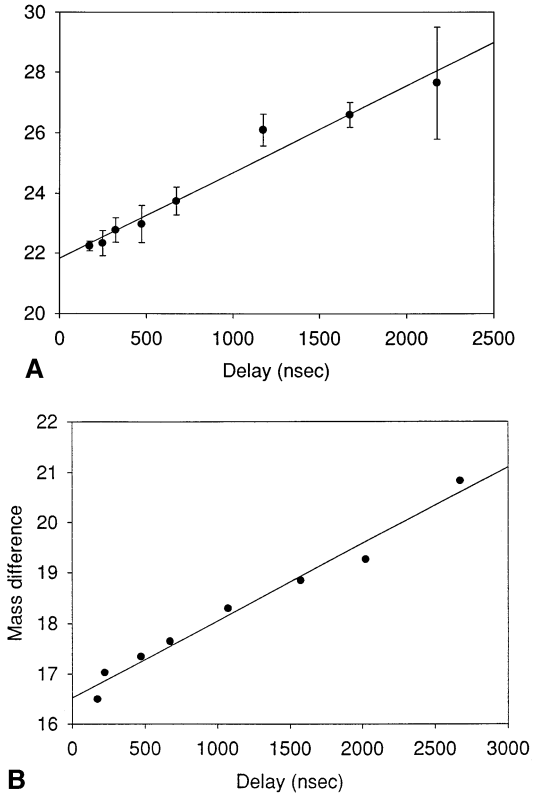

Fig. 7. Graphs showing the increase in mass separation between the focused and unfocused fragment ions for (a) loss of Gal-GlcNAc from the tetra-antennary glycan I recorded from 2,5-DHB and (b) loss of sialic acid in the negative ion spectrum of the ganglioside GM_1 II recorded from 4-HCCA, as a function of source delay.

$$q = 2s_4$$

then

$$M_c = M_a\left[\frac{p + \left(\frac{M_b}{M_a}\right)q}{p + q}\right]^2$$

If $r = q/p$, then

$$M_c = M_a\left[\frac{1 + \left(\frac{M_b}{M_a}\right)r}{(1 + r)}\right]^2 \quad (1)$$

The formula may be rearranged for experimental determination of the instrumental parameter "r" from measured values of M_a, M_b, and M_c

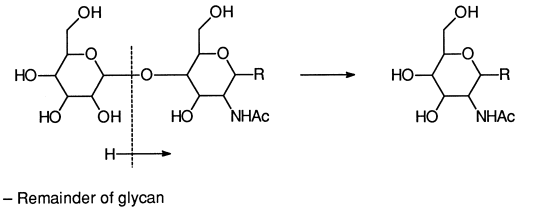

Fig. 8. Y-type fragmentation of the biantennary glycan IV by loss of sialic acid to leave an ion isobaric with that of another native glycan.

$$r = \frac{M_b - M_c + \sqrt{M_c(M_a - 2M_b + M_x)}}{(M_c - M_x)}$$

where

$$M_x = \frac{M_b^2}{M_a}$$

Several sets of precursor and fragment ions were recorded with the various instruments to test the formulae. Table 1 lists the calculated values for the unfocused fragment ion for several fragmentations recorded with four instruments. A good correlation was found in all cases, provided that spectra were recorded, with any particular instrument, under the same conditions in order to keep the value of r constant for that instrument. If the conditions varied, then a new value for r had to be calculated from the above equation, or found experimentally. Fig. 10 shows the effect of delay on the value of r measured for the loss of sialic acid from the ganglioside GM_1 in the Voyager instrument. The precursor and focused fragment ions were isotopically resolved in all examples studied, whereas the metastable fragment ion peak only displayed isotopes when it occurred at relatively low mass (usually less than m/z 1000). Thus, when the poorly focused metastable ion did not display isotopes the spectra were smoothed in order to obtain average masses for all ions.

In addition to being applicable to MALD(I) spectra of carbohydrates recorded with reflectron-TOF mass spectrometers, the formulae were also found to be applicable to other systems such as those used to record the spectrum of the hydrocarbon shown in Fig. 11. This figure shows a field ionization spectrum

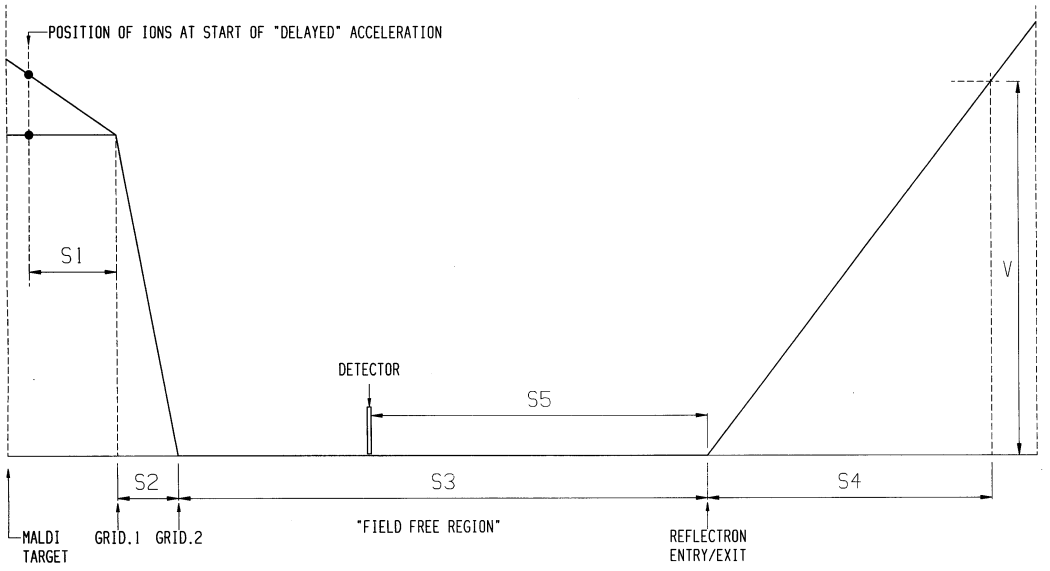

Fig. 9. Plot of the relative electric potentials vs path length for a typical reflectron-TOF mass spectrometer.

recorded from a gas chromatographic inlet to an orthogonal-reflectron-TOF instrument. Calculated metastable masses are shown in Table 1.

3.4.1.1. Precursor ion mass. Formula 1 can be rearranged to obtain the precursor ion (M_a) mass from the masses of the focused and unfocused fragment ion

$$M_a = \left(\frac{M_c}{2}\right)(1 + r)^2 - rM_b + (1 + r) \times \sqrt{\left(\frac{M_c}{2}\right)^2 (1 + r)^2 - rM_bM_c} \quad (2)$$

The precision of mass determination was not as high as with the calculation of the unfocused ion mass because of the relatively large mass separation between the precursor ion and the unfocused fragment ion compared with that between the two fragment ion peaks and the imprecision in centroiding the metastable ion. A difference of 0.1 mass unit in the measurement of the metastable ion mass usually gave an error of about 1 mass unit in the predicted mass of the precursor ion for the loss of sialic acid (291 mass units). However, in use for carbohydrate work, the mass losses are usually in the region of several tens of mass units, thus making this imprecision in the predicted mass relatively insignificant. The value of r was also critical and had to be determined to at least the third decimal place for the formulae to be used accurately. A change of one digit in the third decimal place altered the predicted precursor ion mass by about 1.5 mass units for a mass loss of about 300 mass units. Table 2 shows examples of predicted precursor ion masses using Eq. (2) for several compounds.

3.4.1.2. Fragment ion mass. The fragment ion mass (M_b), predicted from the masses of the precursor and metastable ion masses, is given by rearranging formula (1) to formula (3):

$$M_b = \frac{1}{r}\sqrt{M_cM_a(1 + r) - M_a} \quad (3)$$

This formula can be used to calibrate a PSD spectrum recorded in normal acquisition mode where the ions do not appear at their correct *m/z* values. Thus, Fig. 12 (top) shows the normal PSD spectrum of the high-mannose glycan $(Man)_6(GlcNAc)_2$ (VII) from chicken ovalbumin recorded from 2,5-DHB with the Micromass TOFSpec 2E instrument. Cleavages giv-

Table 1
Comparison of calculated and observed masses of unfocused ions for several carbohydrates recorded with different mass spectrometers

Compd.	Loss	+/−	Mass Type	Mass Parent	Mass Frag.	Unfocused ion Found	Unfocused ion Calc.	Unfocused ion Diff.
Micromass TOFSpec SE, delay = 650 ns, r = 0.857								
A2[a]	Sialic acid	+	Average	2246.8	1955.6	1986.4	1986.1	+0.3
A2[a]	Sialic acid	+	Average	2268.8	1977.7	2008.4	2008.4	0
A2[a]	Sialic acid	+	Average	1955.6	1664.4	1696.7	1696.4	+0.3
A2[a]	Two sialic acids	+	Average	2245.8	1663.9	1742.0	1742.0	0
A2[a]	Sialic acid	−	Average	2222.4	1931.4	1962.4	1962.4	0
Micromass TOFSpec 2E, r = 0.821								
A2[a]	Sialic acid	+	Mono	2246.4	1955.2	1991.0	1991.3	−0.2
A2[a]	Sialic acid	+	Mono	2268.4	1977.3	2013.5	2013.5	+0.1
A2[a]	Sialic acid	+	Mono	1955.3	1664.3	1701.6	1701.7	−0.1
A2[a]	Two sialic acids	+	Mono	2246.4	1664.3	1751.4	1752.2	+0.8
NA4[b]	Gal-GlcNAc	+	Mono	2393.9	2028.7	2077.8	2076.8	+1.0
PerSeptive Voyager Elite, r = 0.954								
GM_1^3 [c]	Sialic acid	+	Average	1569.9	1278.6	1297.6	1298.2	−0.8
GM_1^3 [c]	Sialic acid	+	Average	1597.5	1306.6	1325.6	1326.9	−0.3
GM_2^4 [d]	Sialic acid	+	Average	1434.8	1143.8	1165.2	1164.5	+0.7
A2[a]	Sialic acid	−	Average	2224.1	1932.7	1948.5	1948.5	0
NA4[b]	GalGlcNAc	+	Average	2395.2	2029.4	2051.9	2051.2	+0.7
LST[e]	Sialic acid	+	Mono	1021.9	730.6	757.5	757.1	+0.4
A3[f]	Sialic acid	−	Average	2880.8	2587.6	2603.5	2601.5	+2.0
A3[f]	Two sialic acids	−	Average	2880.8	2298.2	2340.0	2339.7	+0.3
Micromass orthogonal-TOF mass spectrometer, r = 0.641								
$C_{14}H_{30}$	C_2H_5	+	Mono	198.2	169.2	176.2	176.2	0
$C_{14}H_{30}$	C_3H_7	+	Mono	198.2	155.2	166.0	166.0	0
$C_{14}H_{30}$	C_4H_9	+	Mono	198.2	141.2	156.0	156.2	−0.2
$C_{14}H_{30}$	C_5H_{11}	+	Mono	198.2	127.3	146.5	146.7	−0.2

[a]Disialylated biantennary N-linked glycan (III).
[b]Tetra-antennary N-linked glycan (I).
[c]Ganglioside GM_1 (II).
[d]Ganglioside GM_2 (IV).
[e]Sial-Lactose-neo-tetraose (V).
[f]Triantennary N-linked glycan (VI).

ing rise to the fragment ions are outlined in Fig. 13. Below, in Fig. 12, is shown the reflectron-TOF spectrum recorded at high laser power with precursor ion selection. Although very similar, the lower spectrum is not calibrated. However, by applying Eq. (3) to each peak, the correct masses can be obtained as shown in Table 3. A plot of the mass difference between the masses in the PSD spectrum and reflectron-TOF spectrum can be fitted to a second order polynomial and is shown in Fig. 14.

Recording a PSD spectrum as a normal reflectron spectrum with mass selection has the disadvantage that ions are not in focus over the whole mass range as can be seen from Fig. 12(b), hence the need to step

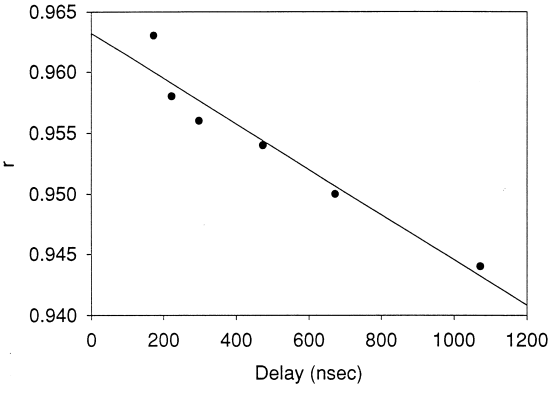

Fig. 10. Effect of delay on the value of r measured for the loss of sialic acid from the ganglioside GM_1 with the Voyager instrument.

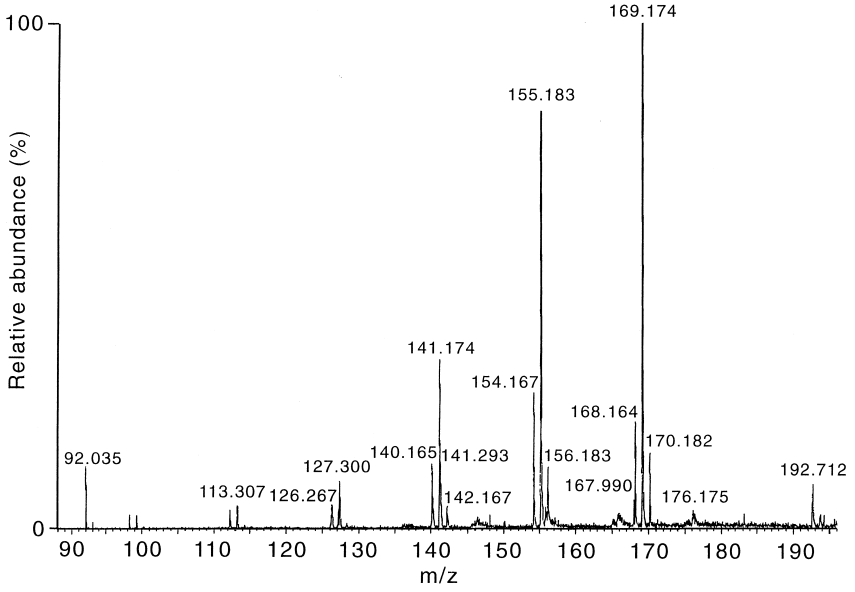

Fig. 11. Field ionization mass spectrum of the hydrocarbon $C_{14}H_{30}$ recorded with a Micromass orthogonal-TOF mass spectrometer.

the reflectron as in Fig. 12(a). However, the stepping routine can lead to quantitative errors between peak intensities as peaks appearing in different segments are not necessarily recorded from the same area of target. For some structural studies, such as isomer differentiation, it is important to determine peak ratios relatively accurately as illustrated by recent work on N-linked glycans by Rouse et al. [16]. This restriction does not apply to the spectrum recorded in normal reflectron mode as in Fig. 12(b). Nevertheless, with sufficient numbers of shots acquired in normal PSD mode, these variations can be averaged out as shown in Fig. 12 where it can be seen that the relative peak intensities are roughly equal. The spectrum in Fig. 12(a) (reflectron stepping) was acquired with 75 laser shots for each segment with the laser spot continually moved over the target surface.

3.5. Use of the formulae to examine the fragmentation pathways occurring in a complex spectrum

A computer program, written in Visual Basic, enabled any of the three ions (precursor, fragment, or metastable) to be calculated given the mass of the other two and was used to examine the fragmentation

Table 2
Predicted parent ion mass for a selection of focused and unfocused fragment ion masses

Instrument	Compound	Mass loss	Delay (ns)	r	Fragment focused	Unfocused	Parent predicted	Found	Error
Micromass TOFSpec 2E	GM_1	Sialic acid	560	0.821	1306.3	1345.8	1598.0	1597.2	−0.8
Micromass TOFSpec 2E	GM_1	Sialic acid	560	0.821	1278.3	1317.7	1568.3	1569.3	+1.0
Micromass TOFSpec 2E	GM_2	Sialic acid	560	0.821	1144.5	1185.3	1436.7	1435.7	−1.0
Micromass TOFSpec 2E	GM_2	Sialic acid	560	0.821	1116.3	1157.1	1407.1	1407.6	+0.6
Voyager	GM_1	Sialic acid	173	0.963	1277.3	1296.0	1570.5	1568.6	−1.9
Voyager	GM_1	Sialic acid	223	0.958	1277.6	1296.5	1566.0	1568.6	+2.6
Voyager	GM_1	Sialic acid	298	0.956	1277.6	1297.1	1569.2	1568.6	−0.6

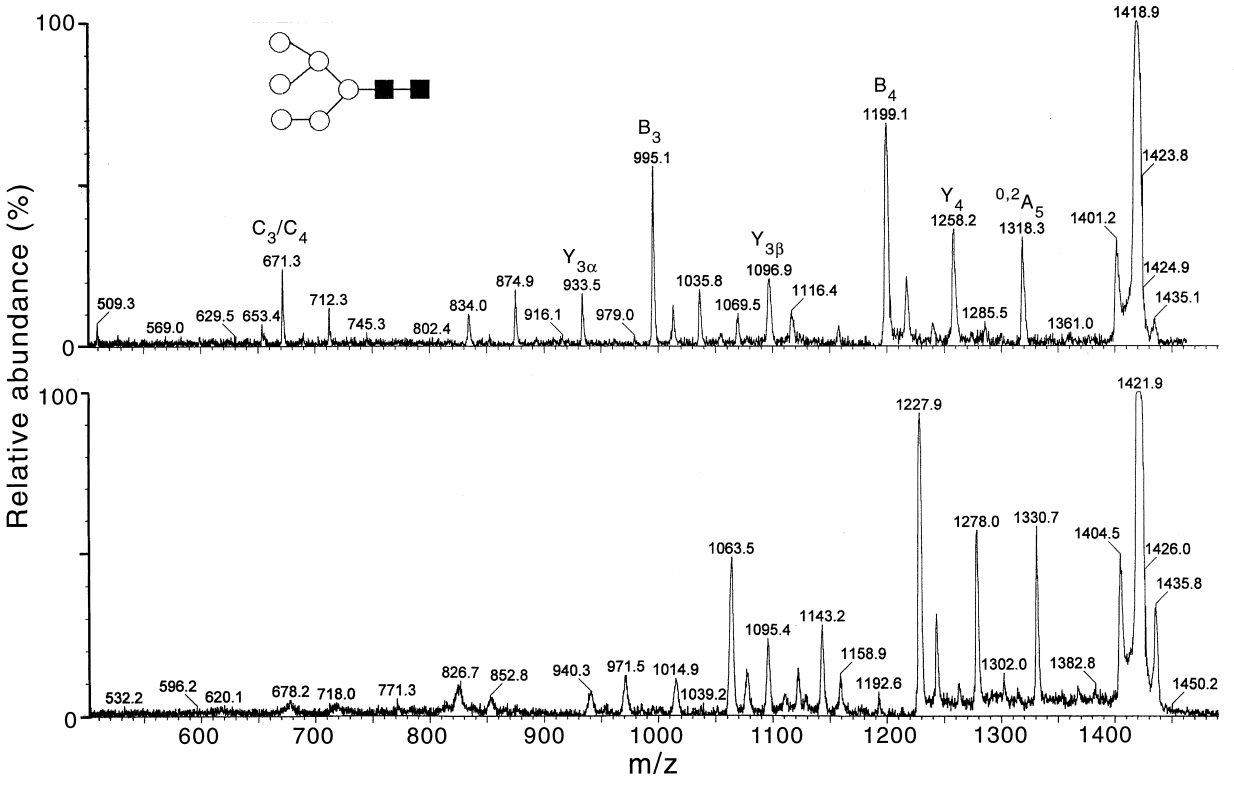

Fig. 12. (a) Positive ion PSD spectrum of the high-mannose glycan $(Man)_6(GlcNAc)_2$ (VII) from ovalbumin recorded from 2,5-DHB with the Micromass TOFSpec 2E instrument. (b) The PSD spectrum obtained by selecting the precursor ion and obtaining a normal reflectron-TOF spectrum with a high laser power.

pattern of glycans displaying fragmentation in their reflectron-TOF spectra. Fig. 15 shows the positive ion MALD(I) spectrum of the disialylated biantennary glycan III recorded with a Micromass TOFSpec SE instrument. Several molecular ions were present because of the tendency of the sugar to form both sodium and potassium salts at each of the carboxylic acid groups of the sialic acid moieties, as seen above with the ganglioside sample. Thus the MNa^+ ion from the free acid was at *m/z* 2245.8 (monoisotopic mass) and the MK^+ ion was at *m/z* 2261.8. Ions from the mono- and di-sodium and potassium salts were at *m/z* 2267.8 ($[M - H + 2Na]^+$), 2289.8 ($[M - 2H + 3Na]^+$), 2283.8 ($[M - 2H + Na + K]^+$), and 2305.8 ($[M - 2H + 2Na + K]^+$) but it is not possible to tell which of the metal ions is the adduct and which is the salt.

The group of ions in the *m/z* 1900–2000 region represent loss of a single sialic acid residue from some of these molecular ions in a Y-type cleavage reaction, together with metastable ions that link these ions to their precursors. Thus, the fragment ion at *m/z* 1954.7 is linked by the metastable ion at *m/z* 1986.4 to the MNa^+ ion of the free disialylated glycan at *m/z* 2245.8 with a value for *r* in Eq. 2 of 0.8491. By using this value, it could be shown that the other metastable fragment ions link the fragments to the precursors shown in Table 4. From this table it can be seen that loss of a single sialic acid moiety can only occur from molecular species in which one of the sialic acids is present as the free acid and not its salt. No fragmentation of the di-metal salts was seen. This supports the proposal that the hydrogen transferred to the ionic fragment from the expelled sialic acid must be that

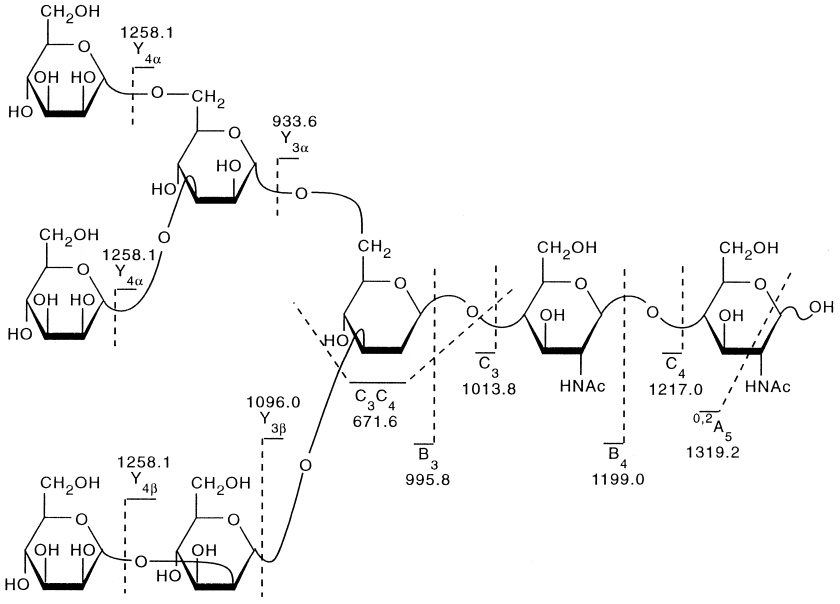

Fig. 13. Formation of the fragment ions in the PSD spectrum of the glycan $(Man)_6(GlcNAc)_2$ shown in Fig. 14. Masses are average.

from the carboxylic acid group. Similarly, the fragment ion at *m/z* 1911.0, which has lost both carbon dioxide and sialic acid, arises by loss of sialic acid from the in-source fragment that has lost carbon dioxide (*m/z* 2201.8).

The single fragment ion arising by loss of two sialic acid groups (*m/z* 1663.9) was accompanied by two metastable ions (*m/z* 1696.2 and 1741.9) indicating that it was formed by two fragmentation routes. The metastable ion at *m/z* 1696.2 indicates the in-source fragment ion at *m/z* 1954.7 as the precursor whereas the metastable ion at *m/z* 1741.9 shows simultaneous loss of two sialic acids from the ion at *m/z* 2245.8 by post-source decay. The precursor ion for this fragmentation was also that for the formation of the in-source fragment at *m/z* 1954.7. Thus, the

Table 3
Mass differences between the PSD ions recorded in reflectron and PSD mode for the glycan $(Man)_6(GlcNAc)_2$ from ovalbumin

True mass	Reflectron mass	Mass difference	Mass from formula 3	Mass difference (Calc:true)	PSD mass	Mass difference (PSD:true)
1402.2	1404.6	2.4	1402.8	+0.6	1401.2	−1.0
1319.2	1330.7	11.5	1319.3	+0.1	1318.3	−0.9
1258.1	1278.0	19.9	1258.3	+0.2	1258.2	+0.1
1199.0	1228.1	29.1	1199.4	+0.4	1199.1	+0.8
1096.0	1143.2	47.2	1096.4	+0.4	1096.9	+0.9
1036.9	1095.4	58.5	1036.6	−0.3	1035.8	−1.1
995.8	1063.5	67.7	996.1	+0.3	995.1	−0.7
933.8	1014.9	81.1	933.0	+0.3	933.5	−0.3
874.8	970.5	95.7	874.1	−0.8	874.9	+0.1
833.7	941.1	107.4	834.4	−0.7	834.0	+0.3
712.6	852.8	140.2	711.1	−1.5	712.3	−0.3
671.6	826.7	155.1	673.5	+1.9	671.3	−0.3

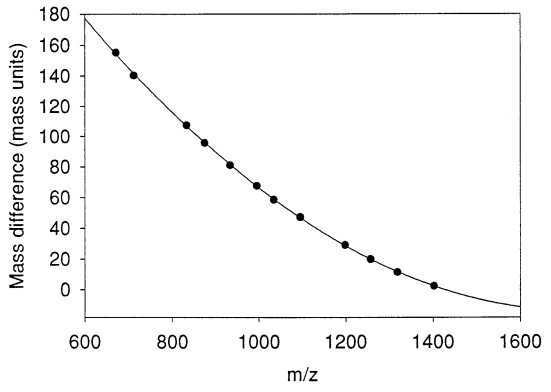

Fig. 14. Plot of the mass difference between PSD ions recorded by stepping the reflectron voltage and by keeping the voltage constant for the high mannose glycan $(Man)_6(GlcNAc)_2$.

desialylated fragment at *m/z* 1663.9 originated from *m/z* 2245.8 by two mechanisms: a two-stage process in which sialic acid was lost as an in-source fragmentation to give *m/z* 1954.7 which then decayed in a PSD fragmentation, and a single-stage process whereby both sialic acids were lost by PSD. None of the ions containing salts were able to form *m/z* 1663.9 as they did not possess a labile acidic hydrogen atom. These fragmentations are outlined in Fig. 16.

Another set of low abundance ions was present between *m/z* 1136 and 1663. The ion at *m/z* 1298.7 was formed by loss of Gal-GlcNAc (365.1 mass units) from the ion at *m/z* 1663.9 as shown by the presence of the metastable ion at *m/z* 1345.4. A second metastable ion at *m/z* 1335 predicted a second precursor ion in the region of *m/z* 1590. An ion was present at 1589.5 corresponding to a cross-ring cleavage resulting in loss of C4–C6 from a hexose residue of the ion producing the peak at *m/z* 1663.9. A metastable ion could not be found for this fragmentation, consistent with earlier observations [10] that such cross-ring fragmentations are fast processes and occur in source. This fragmentation can only represent loss of C4–C6 from either a terminal galactose residue or from one of the mannose residues. The fragment at *m/z* 1427.5 was formed by loss of galactose (162 mass units) from this cross-ring fragment. Finally, the fragment at *m/z* 1136.6 was formed by loss of galactose from the ion that had lost Gal-GlcNAc (*m/z* 1298.7, metastable ion peak of low intensity at *m/z* 1154) and also by loss of 291 mass units (GlcNAc plus C1–C3 from the galactose that had lost 74 mass units above). These fragmentations are outlined in Fig. 17.

3.6. Use of formula (2) to predict the mass of a precursor ion missing from the MALD(I) spectrum

Loss of anionic groups from some glycans occurs so readily that only fragment ions are present in the spectra. An example of this was encountered in the positive ion spectrum of a biantennary glycan containing a uronic acid, a neuraminic acid, and two sulphate groups, derivatised as its 2-aminobenzamide (2-AB) derivative (Fig. 18). The calculated monoisotopic mass of this compound is 2599.8 (MNa^+) but no ion of this mass, or of that of any sodium or potassium salts, was present in the spectrum. The focused fragment ion at *m/z* 2146.9 together with the unfocused ion at 2162.6 confirmed loss of the sialic acid from the fragment ion at *m/z* 2437.9. The second unfocused fragment ion at *m/z* 2178.7 suggested a second pathway for the formation of the fragment ion at *m/z* 2146.9 in a comparable manner to the two routes leading to the fragment at *m/z* 1664.3 in Fig. 16. Spectra were smoothed to give average masses and the predicted mass for this second precursor ion, given by Eq. 2, was found to be *m/z* 2621.2. This mass corresponds closely to the calculated average mass of *m/z* 2623.3 for the monosodium salt of the expected disulphated structure (the predicted error, based on the uncertainty in the centroid of the metastable ion peak of about ± 0.5 mass units, is about ± 3 mass units). Later experiments using exoglycosidase digestions confirmed the composition of the glycan as given above. Further details of this structure will be published later.

Although this appears to be the first example of the use of metastable ions to predict the mass of an absent precursor ion in MALD(I) spectra, it should be noted that absent precursor ions have previously been detected in magnetic sector instruments by use of metastable ions by changing the instrumental focusing conditions [21].

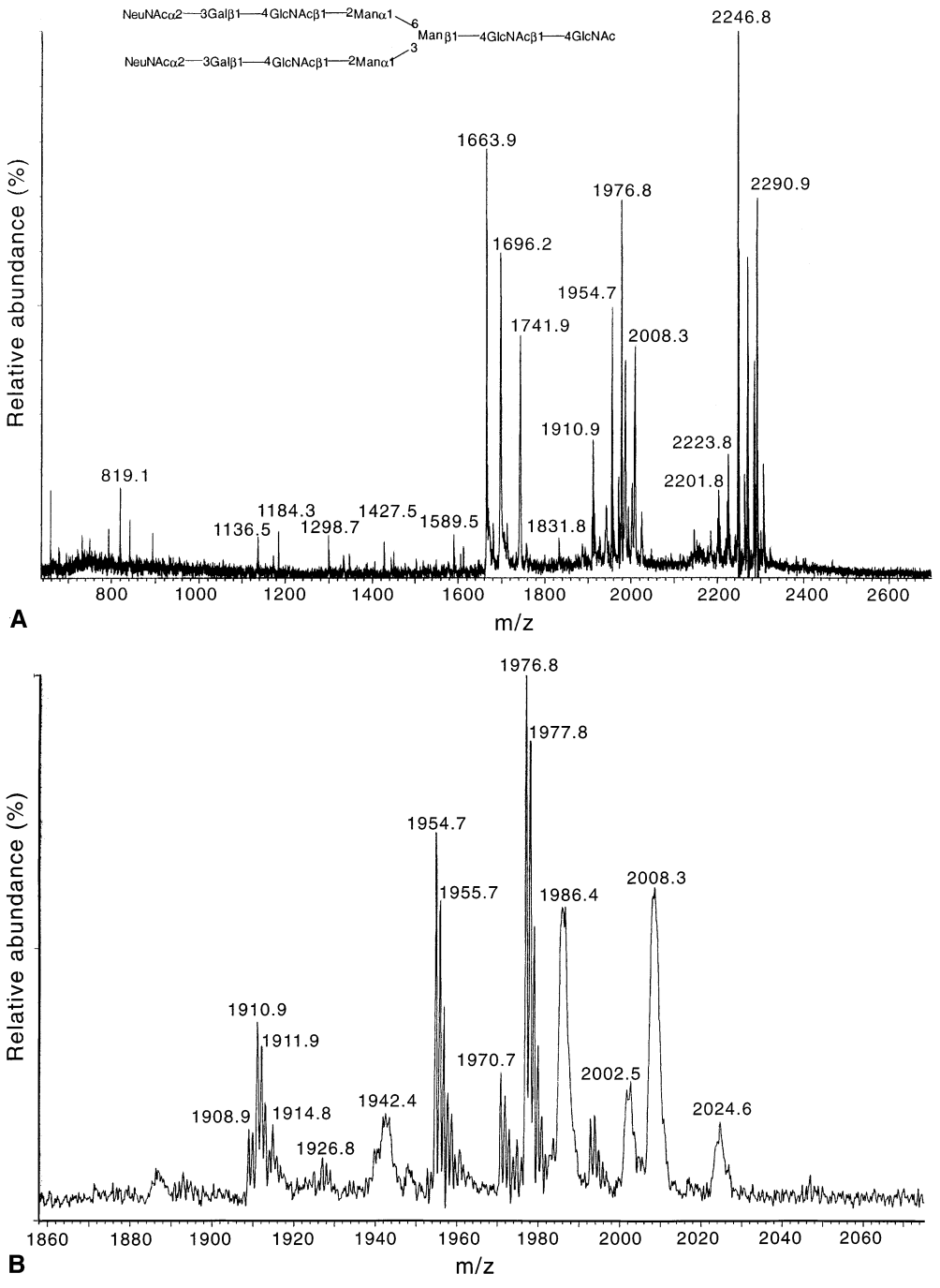

Fig. 15. (a) Positive ion MALD(I) mass spectrum of the disialylated biantennary N-linked glycan III recorded from 2,5-DHB. (b) Expanded region corresponding to ions formed by loss of a single sialic acid.

Table 4
Relationship between the focused and metastable fragment ions and the precursor ions in the positive ion MALD(I) mass spectrum of the disialylated biantennary N-linked glycan III

Fragment (*m/z*)	Metastable (*m/z*)	Predicted precursor ion (*m/z*)[a]	Found (*m/z*)	Ion
1992.8	2024.6	2285.6	2283.8	X + Na + K
1976.8	2008.3	2266.9	2267.8	X + 2Na
1970.7	2002.5	2262.2	2261.8	X + K
1954.7	1986.4	2245.8	2245.8	X + Na
1911.0	1942.4	2198.6	2201.8	X + Na − CO_2
1663.9	1696.2	1950.7	1954.7	Y
1663.9	1741.9	2238.5	2245.8	Y

[a]From formula (2).

4. Conclusions

PSD ions generated in MALD(I) spectra recorded with reflectron-TOF mass spectrometers fitted with time-lag focusing are observed in the normal spectra as unfocused ion peaks appearing a few mass units higher than the position of the focused ions. This is because they leave the ion source at the velocity of the precursor and, thus, after fragmentation in the first field-free region, arrive at the reflectron after the corresponding in-source fragment. These ions, therefore, never catch up with the in-source fragments and, thus, arrive later at the detector giving the appearance of higher mass. This behaviour is unlike that of metastables observed in magnetic sector instruments that are observed at lower mass than that of the fragment. Again, unlike the situation in magnetic sector instruments, the apparent mass of the metastable ions is dependent on the instrument geometry and ion-source focusing conditions. An equation linking the masses of the three ions (precursor, focused

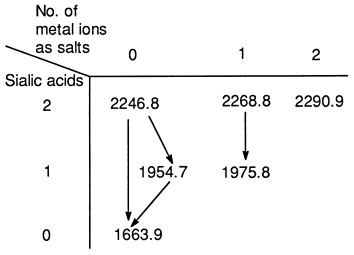

Fig. 16. Scheme showing the fragmentation pathways involving loss of sialic acid for the disialylated biantennary glycan IV.

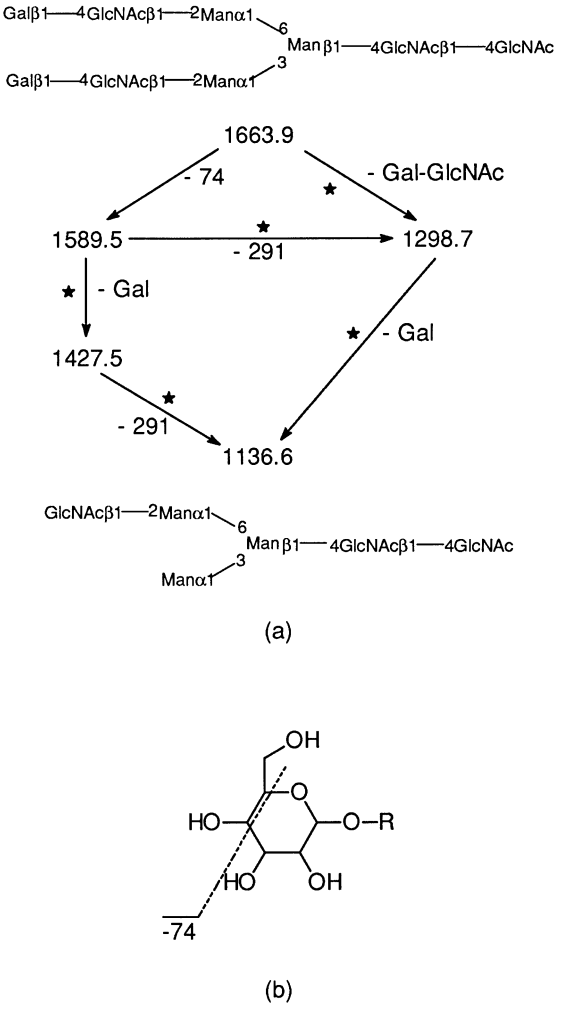

Fig. 17. (a) Scheme showing fragmentation of the antennae of the fragment ion at *m/z* 1663.9 in the mass spectrum of the disialylated biantennary glycan IV. Stars are metastable ions observed. (b) Loss of 74 mass units from a hexose residue.

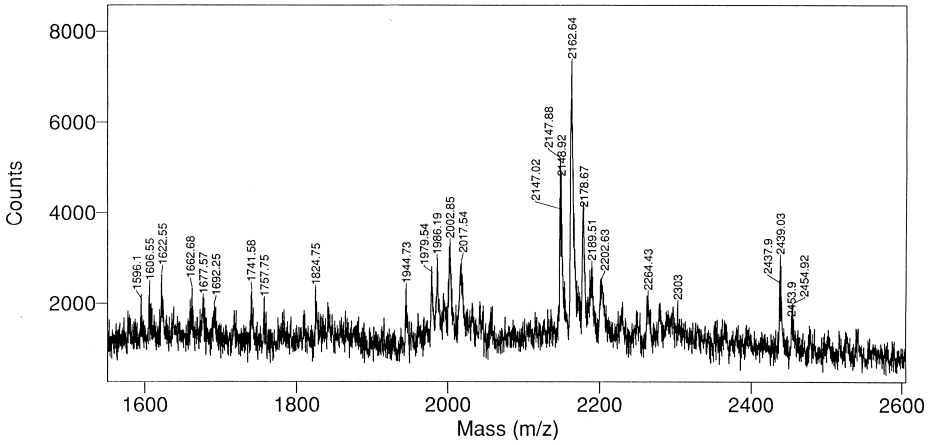

Fig. 18. Positive ion MALD(I) mass spectrum of a tetra-acidic analogue of the biantennary glycan.

fragment, and metastable) that contains a term reflecting the instrumental parameters has been developed and, because this term is instrument-dependent, the equations can be used with any TOF mass spectrometer. The formulae can be used to investigate fragmentation mechanisms and to predict the mass of an unstable molecular ion that is absent from a spectrum.

Acknowledgements

We thank Professor R.A. Dwek, Director of the Glycobiology Institute, for his help and encouragement. We also thank Drs. S. Zamze and D.R. Wing for permission to use the preliminary data from the tetra-anionic glycan discussed in Sec. 3.6. This work was supported, in part, by a grant from the Biotechnology and Biological Sciences Research Council.

References

[1] K.K. Mock, M. Davey, J.S. Cottrell, Biochem. Biophys. Res. Commun. 177 (1991) 644.
[2] P. Juhasz, C.E. Costello, J. Am. Soc. Mass Spectrom. 3 (1992) 785.
[3] D.J. Harvey, J. Mass Spectrom. 30 (1995) 1311.
[4] D.J. Harvey, J. Chromatogr. A 720 (1996) 429.
[5] D.J. Harvey, in Glycopeptides and Related Compounds: Synthesis, Analysis and Applications, D.G. Large, C.D. Warren (Eds.), Marcel-Dekker, New York, 1997, pp. 593–628.
[6] D.J. Harvey, B. Küster, T.J.P. Naven, Glycoconjugate J. 15 (1998) 333.
[7] B. Stahl, M. Steup, M. Karas, F. Hillenkamp, Anal Chem. 63 (1991) 1463.
[8] D.J. Harvey, P.M. Rudd, R.H. Bateman, R.S. Bordoli, K. Howes, J.B. Hoyes, R.G. Vickers, Org. Mass Spectrom. 29 (1994) 753.
[9] K. Strupat, M. Karas, F. Hillenkamp, Int. J. Mass Spectrom. Ion Processes 111 (1991) 89.
[10] T.J.P. Naven, D.J. Harvey, J. Brown, G. Critchley, Rapid Commun. Mass Spectrom. 11 (1997) 1681.
[11] M.C. Huberty, J.E. Vath, W. Yu, S.A. Martin, Anal. Chem. 65 (1993) 2791.
[12] B. Spengler, D. Kirsch, R. Kaufmann, J. Lemoine, Org. Mass Spectrom. 29 (1994) 782.
[13] D.J. Harvey, T.J.P. Naven, B. Küster, R.H. Bateman, M.R. Green, G. Critchley, Rapid Commun. Mass Spectrom. 9 (1995) 1556.
[14] J. Lemoine, F. Chirat, B. Domon, J. Mass Spectrom. 31 (1996) 908.
[15] R. Kaufmann, P. Chaurand, D. Kirsch, B. Spengler, Rapid Commun. Mass Spectrom. 10 (1996) 1199.
[16] J.C. Rouse, A.-M. Strang, W. Yu, J.E. Vath, Anal. Biochem. 256 (1998) 33.
[17] T. Patel, J. Bruce, A. Merry, C. Bigge, M. Wormald, A. Jaques, R. Parekh, Biochemistry 32 (1993) 679.
[18] D.J. Harvey, Rapid Commun. Mass Spectrom. 7 (1993) 614.
[19] J.H. Beynon, Mass Spectrometry and its Applications to Organic Chemistry, Elsevier, Amsterdam, 1960.
[20] B. Domon, C.E. Costello, Glycoconjugate J. 5 (1988) 397.
[21] L.A. Shadoff, Anal. Chem. 39 (1967) 1902.